# Bio-based Tannin-Furanic-Silk Adhesives: Applications in Plywood and Chemical Crosslinking Mechanisms

*Emanuele Cesprini[1], Johannes Jorda[2] ,Marco Paolantoni[3], Luca Valentini[4], Primoz Sket[5], Valerio Causin[6], Diana E. Bedolla[7,8], Michela Zanetti[1] and Gianluca Tondi[1*]*

[1] TESAF Land Environment Agriculture & Forestry Department, University of Padua, Viale dell'Università 16, 35020 Legnaro, Italy; emanuele.cesprini@phd.unipd.it (E.C.); michela.zanetti@unipd.it (M.Z.); gianluca.tondi@unipd.it (G.T)

[2] Department of Green Engineering and Circular Design, Salzburg University of Applied Sciences, Markt 136a, 5431 Kuchl, Austriajohannes.jorda@fh-salzburg.ac.at (J.J)

[3] Department of Chemistry, Biology and Biotechnology, University of Perugia, Via Elce di Sotto 8, Perugia, 06123, Italy. (M.P)

[4] Civil and Environmental Engineering Department, University of Perugia, Strada di Pentima 4, Terni, 05100, Italy. luca.valentini@unipg.it (L.V); marco.paolantoni@unipg.it (M.P)

[5] Slovenian NMR Centre, National Institute of Chemistry, Hajdrihova 19, SI-1000 Ljubljana, Slovenia. primoz.sket@ki.si (P.S)

[6] Department of Chemical Sciences, University of Padua, Via Marzolo 1, 35131 Padova, Italy;
valerio.causin@unipd.it (V.C)

[7] Elettra Sincrotrone Triete, S.S.14 Km 163.5 in Area Science Prk, 34149 Basovizza, TS, Italia

[8] Area Science Park, Padriciano 99, 34149 Padriciano, TS, Italia

diana.bedolla@elettra.eu (D.B)

* Correspondence: gianluca.tondi@unipd.it; Tel.: +39-049-8272776

KEYWORDS. Regenerated silk; Protein; Fibroin, Flavonoids; Furanic; Engineered wood products; sustainable.

## ABSTRACT

Due to their abundance in nature, their commercial availability, and their reactivity, wood polyphenolic extracts commonly called tannins are excellent candidates for the production of bioplastics. In particular, they were tested as wood adhesives with several hardeners but their low moisture resistance and their rigidity reduced their technological interest. In the present study, we combined regenerated silk (RS) with the tannin-furanic formulations to improve their properties. Three-layer plywood glued with these several fully-renewable tannin-silk-furanic adhesives were tested for their mechanical properties: the modulus of elasticity, the modulus of rupture, and both dry and wet shear strength were enhanced when 20 wt% of RS was added. Initially, the cross section of the prepared samples was investigated by scanning electron microscopy, indicating a

good dispersion of RS within the tannin-furanic matrix. Afterward, thermomechanical analysis of the adhesive has highlighted that RS slows down the polymerization rate, decreasing the cross-linking kinetics of poly-furfuryl alcohol. Chemical investigations through ATR FT-IR and $^{13}$C-NMR show the formation of covalent bonds between RS and the furanic matrix. In summary, the combination of bioresources from the vegetal and animal kingdom allows the manufacturing of fully bio-based adhesives with enhanced mechanical properties and water resistance. This represents an important breakthrough in the exploitation of polyphenols, opening new perspectives for their application in material science.

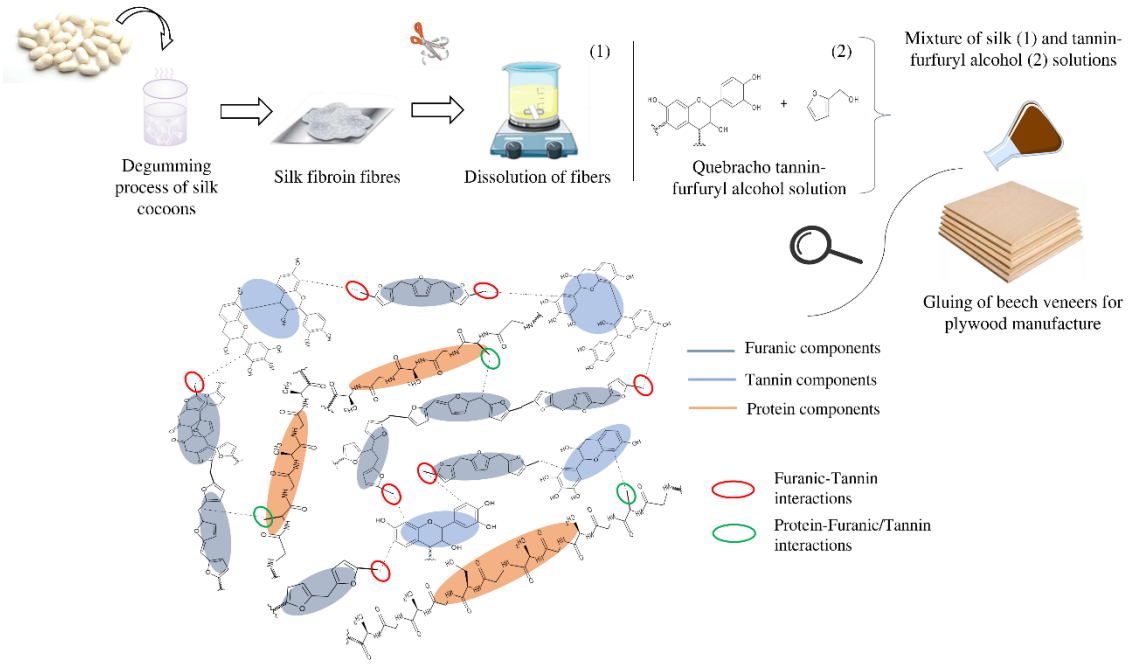


## INTRODUCTION

Reducing the dependence on fossil derivatives has become a worldwide issue due to the necessity to restrain global warming and develop a sustainable economy [1]. For instance, the plastics field accounts for 5-7% of the consumption of oil derivatives, releasing more than 850 million tons of $CO_2$ into the atmosphere[2]. Specifically, the higher GHG's emissions in the plastic manufacturing

industry are related to the raw material extraction process (e.g. 61%) followed by the polymer production (e. g. 30%).[3] It has been estimated that replacing approximately 66% of conventional plastics with bio-based alternatives would avoid between 241 and 316 $MtCO_2$ equivalents per year[4]. Thus, explaining the need to seek sustainable alternatives to oil derivatives. Although the most common commercial plastics are still made from oil derivatives, the same materials may also be replaced by renewable resources. Monomers or also biopolymers can be obtained from nature with the goal of replacing synthetic plastic such as polyethylene (PE) or polypropylene (PP).[5] Tannins, which are wood extracts of polyphenolic nature, have been shown to be very attractive and perform for multiple purposes. These substances are produced by plants to protect the lignocellulosic body against biological and radiation attacks, due to their chemical structure and antioxidant capacity.[6] Furthermore, they have a 'green' extraction process through the use of water as a solvent under moderate pressure and temperature.[7] Tannins are extracted industrially and are therefore abundantly available because they were and are used as tanning agent in the leather tannery row because of their strong complexing power with proteins.[8] In addition to this, tannin extracts have been used for medical purposes as antioxidants and free radical scavengers.[9] In the last two decades, due to their appealing chemical features, tannins have been used to produce biobased plastics, with particular interest for insulation foams[10–12] wood preservatives[13,14] and wood adhesives.[15,16] The addition of mainly synthetic-based cross-linkers such as hexamine, formaldehyde or glyoxal, lead to stable three-dimensional thermosetting polymers.[17,18] Despite the appealing features of the aforementioned tannin-based formulation, the concerns about health problems and the need for detachment from oil derivatives, lead the research to promote free-formaldehyde fully renewable formulations, as profitable source for greener products. In this direction, furfuryl alcohol is bio-derived material which is mainly obtained from the hydrogenation

of furfural, itself a derivative of the dehydration of agricultural and forest waste from hemicelluloses.[19] The ability of furfuryl alcohol to self-cure under acidic conditions [20,21] enables the design of different materials applicable in the field of engineered wood products, including impregnation [22] and modification [23]of woody material. Moreover, due to the resistance to acid, alkali, high temperature, fungal attack, corrosion [24]and because of its good interaction capacity with tannins[25], furfuryl alcohol can be involved as green crosslinker to produce fully renewable co-polymer.[26,27]However, some critical drawbacks of furanic-tannin co-polymers like poor moisture resistance[28] and high rigidity[29] still limit the application. Hither, proteins have attracted great attention due to their renewability, effortless modification, biodegradability and abundance [30]. Although the use of protein-based adhesive resins alone does not allow for high performance [31], the combination of those with other resources, as tannins or furanic derivates, led to satisfactory results in the wood adhesive sector.[32,33] Silk fibroin (hereinafter named regenerated silk, RS), is one of the most promising natural protein-based biomaterials due to its inspiring biodegradability, and superior mechanical performances.[34] Such biopolymer recovered from insect farming (i.e *Bombyx mori* (e. g. *B. mori*) silkworms) can be processed in solution to enable the fabrication of adhesives with tunable mechanical properties[35], opening up new alternatives to the main plant proteins currently proposed [36,37]

In this study, the effect of adding different amounts of RS into tannin-furfuryl alcohol formulations for plywood manufacturing was investigated. Further, the interaction between the components of the adhesive were observed during and after curing through thermomechanical analysis and solid state $^{13}$C-NMR FTIR spectroscopies.

## MATERIALS AND METHOD

### Materials

Quebracho (*Schinopsis balancae*) tannin extract (Fintan 737B) was kindly provided by the company Silvateam (S. Michele Mondovì, Cuneo, Italy) while furfuryl alcohol (99%) by International Furan Chemical IFC (Rotterdam, The Netherlands). Lowest grade Bombyx mori silk cocoons was provided by a local company (CREA-AA, Padova, Italy). Sodium hydrogen carbonate, calcium chloride, and formic acid were supplied by Alfa Aesar (Thermo Fisher, Waltham, MA, USA). Pre-conditioned (20°C, 65% relative air humidity) rotary cut defect-free beech (*Fagus sylvatica*) veneers, purchased from Europlac (Topolcany, Slovakia), with a nominal thickness of 2.2 mm, density of 0.72 g/cm$^3$ and 12% m.c., were used to prepare the three-layers plywood.

### Synthesis of adhesive

The silk fibers dissolution method was carried out according to previous work.[38] Briefly, *B. Mori* silk cocoons (5g) were degummed in boiling water (300 mL) at 1.7% of $NaHCO_3$ for 30 min and flushed with deionized water, the procedure was repeated twice. The degummed silk fibers were dried at room temperature under air flux, and thus dispersed into the formic acid/calcium chloride solution by magnetic stirring at room temperature for 5 min, until a homogeneous solution was obtained. The amount of calcium chloride was defined in function of silk content. Thus, the silk-calcium chloride weight ratio was set at 70:30, while a silk concentration of 0.11 g/mL in formic acid was chosen. Meanwhile, a tannin-furfuryl alcohol solution was prepared at room temperature and under mechanical stirring, at the fixed weight ratio of 60:40. Afterwards, the two solutions were mixed and mechanically stirred at different RS concentrations calculated on fixed solid

tannin content, obtaining different tannin-furfuryl alcohol formulations (TFS). The RS content was varied from 10wt% up to 30wt%. The composition of the formulations is reported in table1.

**Table 1.** Relative content of each component within the final formulations.

| Samples | Tannin (wt%) | Furfuryl Alcohol (wt%) | RS (wt% on tannin) |
|---|---|---|---|
| TFS-0 | 60 | 40 | / |
| TFS-10 | | | 10 |
| TFS-15 | | | 15 |
| TFS-20 | | | 20 |
| TFS-30 | | | 30 |

Plywood manufacturing

The plywood lay-up consisted of three layered 90° crosswise oriented 2.2 mm thick beech veneers. Adhesive application was carried out manually by weighing 200 g/m$^2$ of adhesive per glue line. Pressing was conducted using a Höfler HLOP 280 (Taiskirchen, Austria) hot press. The pressing conditions were set as follows: pressure of 3 N/mm$^2$, temperature 125°C and 15 minutes of pressing time. The as prepared boards were stored until constant weight in a climate chamber at 20°C and 65% of relative humidity. Test specimens were cut from the plywood boards for the determination of bending strength (MOR), stiffness (MOE), and dry and wet tensile shear strength (SS).

Mechanical characterization

Dry state SS and 24 h water soaking TSS were determined according to EN 314:2004[39] with specimen dimensions 100 mm x 25 mm. Modulus of rupture and MOE were determined by a three-point bending test according to EN 310:1993 with specimen dimensions 250 mm x 50 mm.[40]. All

mechanical properties (SS, MOE, and MOR) were determined using a Zwick/Roell 250 8497.04.00 universal testing machine (Ulm, Germany).

SEM

The morphological characterization of the adhesives was performed by scanning electron analysis with FEI Quanta scanning electron microscopy (variable pressure environmental E/SEM). The instrument is also equipped with EDX (EDAX Element- C2B) for X-ray detection. The images were recorded at 20 kV.

Thermomechanical analysis (TMA)

Thermomechanical analysis was carried out with a TMA/SDTA840 Mettler Toledo (Mettler Toledo, Columbus, OH, USA) instrument equipped with a three-point bending probe. About 20 mg of tannin-based formulations (TSF-0, TFS-10, TFS-15, TFS-20, TFS-30) were applied between two beech wood plies (15 mm × 5 mm × 1.5 mm). Isothermal and non- isothermal methods were applied: the former was run at 25°C for 240 min, while the latter consisted of 10 °C/min heating rate from 40°C to 200°C. For both methods a cycle of 0.1/0.5 N force was applied on the specimens, with each force cycle lasting 12 s (6 s/6 s).

In order to investigate the chemical bonding evolution, different spectroscopic investigations were performed on polyfurfuryl alcohol (PFA) crosslinked in formic acid, regenerated silk (RS) obtained by dissolution in formic acid, PFA-RS and PFA-RS-quebracho tannin (PFA-RS-T) were acquired and compared with the cured mixed formulation subject of this study.

$^{13}$C-NMR solid state analysis

Solid-state $^{13}$C-NMR experiments were performed on a Bruker AVANCE NEO 400 MHz NMR spectrometer using a 4-mm CP-MAS probe. The sample spinning frequency was set to 15 kHz experiments consisted of excitation of protons with p/2 pulse of 3.0 s, CP block of 2 ms, and signal

acquisition with high-power proton decoupling. A total of ca. 2,000 to 14,000 scans were accumulated with the repetition delay of 5 s.

ATR-FTIR analysis

Fourier transform infrared (FTIR) spectra measurements were done in Attenuated Total Reflection (ATR) mode using an Alpha (Bruker Optics) spectrometer equipped with a Platinum ATR module. The spectra were registered in the range between 400 and 4000 $cm^{-1}$, averaging over 30 scans with a resolution of 2 $cm^{-1}$. The spectra were then baseline corrected, normalized and smoothed with the RStudio Team (2021) software.

FTIR

FTIR hyperspectral images were acquired by using a bidimensional 64x64 pixels focal plane array (FPA) coupled to a VIS-IR microscope Hyperion 3000 (Bruker Optics, Billerica, US) and with a VERTEX 70v in-vacuum interferometer (Bruker Optics, Billerica, US) through a 15x Cassegrain objective-condenser pair in transmission mode. Slices of 10 um of PFA-tannin and PFA-tannin-silk were prepared with a rotary microtome (Leica RM2245; Leica Biosystems, Nussloch, Germany),so that the samples could be measured in transmission mode. For each tile 4096 spectra were acquired with 256 scans at a spectral resolution of $4cm^{-1}$. Data were corrected for water vapor using Opus 8.5 SP1 (Bruker Optics, Billerica, US) and then analyzed using Quasar (https:\\quasar.codes). [41,42] All spectra were vector normalized, cut in the region 1850-850 $cm^{-1}$ and baseline corrected with the rubber band correction. Integration was calculated on the average spectra of the whole tile (4096 scans) of each sample with the height of the band around 1715 and the band around 1520. Finally, its ratio was estimated and compared.

Statistical analysis.

Analysis of variance was used to assess significant differences between the investigated formulations through one-way ANOVA and Kruskal test, depending on whether the data are normally or non-normally distributed, respectively. Any groups that showed a significant difference were discriminated according to the Tukey multi-range test for ANOVA or to Dunn test for Kruskal, and a 95% confidence level was selected. Statistical analysis was performed using RStudio Team (2021). Kruskal-Wallis multiple comparison p-values was carried out to analyze the correlation between MOR of the fabricated adhesives, because of non-normal data distribution.

## RESULT AND DISCUSSION

The mechanical properties of the three-layer plywood are depicted in figures 1 A and 1 B. In the production of multilayer panels, one of the key parameters refers to the glue line property, which shall guarantee sufficient adhesion for the final stability of the panel. The most significant physical indicator is the shear strength in both wet and dry conditions (Figure 1A). One-way ANOVA reported high correlation between the silk concentration and $SS_{dry}$ (p-value = $6.29 \cdot 10^{-5}$). Specifically, a significant difference (p-value<0.05) between the reference panels (TFS-0) and TFS-15/20/30 is highlighted by Tukey test, confirming the higher adhesive property of the TFS-20 sample (e. g. 3.2 MPa). In contrast, any substantial difference between TFS-0 and TFS-10 (p-value = 0.052) was not observed.

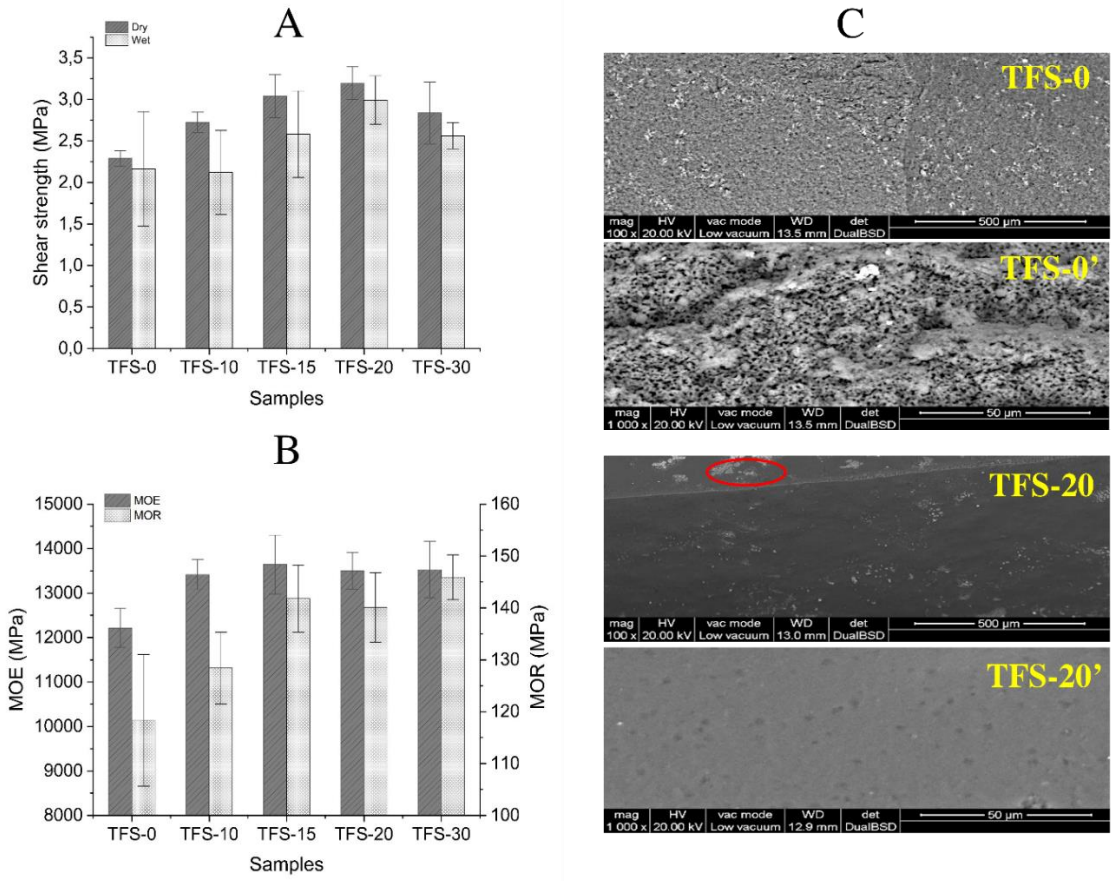


**Figure 1.** A: Dry and 24h wet shear strength of reference panels (TSF-0) and TFS samples synthesized at different wt% of RS. B: Modulus of elasticity (MOE) and modulus of rupture (MOR) of reference panels (TFS-0) and TFS samples synthesized at different wt% of RS. C: Scanning electron microscopy images of TFS-0, TSF-20 and of TFS-0', TSF-20' samples, at different magnifications (e. g. x100 and x 1000, respectively).

After 24 h of water storage at room temperature, the shear stress was evaluated and the tendency is reported by the red curve in Figure 1A. The addition of RS to tannin-furfuryl alcohol matrix led to an increase in panel stability (p-value = 0.0261), reaching its highest value (eg 2.8 MPa) for the TFS-20 formulation. A proportional increase in tensile shear strength is achieved up to 20% of RS,

followed by a decrease when the RS concentration reaches 30%. Although the stability of the adhesive reaches its best properties at 20wt% of RS, the results obtained are all compliant for dry condition purposes according to the European standards that set the wet shear strength above 1 MPa[39]. The effect of RS addition on both MOE and MOR was investigated and reported in Figure 1B. The addition of RS increases the values of both the MOE and MOR. Specifically, the RS addition affects the MOE (p-value = 0.0144), showing a significant change between the reference panels (TSF-0) and those where RS was added (p-value < 0.05). Otherwise, no differences in MOE were highlighted by increasing the RS content (p-value>0.05). Finally, the silk addition positively affects the mechanical properties, registering a p-value of 0.0043 for MOR. Similarly, when silk was added, an increase of the MOR from 128 MPa to 146 MPa was recorded, respectively.
Focusing on the critical tensile shear strength parameter, the comparison of the current formulations with literature studies highlighted the competitiveness of this adhesive resin.

In particular, the use of fully renewable tannin-furfural adhesives showed poor moisture resistance.[29] Indeed, although a dry shear stress strength between 1.7 MPa and 2.3 MPa is registered, the formulation denoted no resistance to moisture due to the panels delamination during the 24h water soaking for plywood EN 314 class 1 application.[29] The grafting of counterparts to the tannic base skeleton is therefore necessary to achieve competitive properties. In this way, the inclusion of oxidized glucose to mimosa tannin allowed dry SS between 1.4 MPa – 2.0 MPa, increasing the moisture resistance until 0.3-0.5 MPa after 24 hour water soaking.[43] Chen et al. report a wet tensile shear strength of 1.1 MPa for soybean meal flour, larch tannin and triglycidylamine adhesive formulation.[44] Similar results are reported by Zhou et al.,[45] who have achieved a dry and wet shear strengths of 2.1MPa and 1.6 MPa, respectively, building a complex structure of layered double hydroxide (LDH), anchored chicken feather fiber (CFF), tannic acid

232 (TA) and soybean meal (SM). The combination of polyfurfuryl alcohol with gluten proteins
233 showed good bonding properties, achieving a shear strength after 24 in cold water of about 0.9
234 MPa [32]. Good strength is also reported for 3 hours in boiling water[32].
235 Another interesting natural resource of polyphenolic character is lignin, which is also used in
236 combination with different kind proteins to produce plywood boards. On this wise, Pang et al.[46]
237 and Liu et al.[47] reported a lower values of both $SS_{dry}$ and $SS_{wet}$ than the results reached by the
238 proposed tannin silk formulation, which displayed to be competitive with PF bonded plywood
239 too.[48]
240 Moreover, in terms of MOE and MOR the current formulation has shown properties comparable
241 with the main synthetic adhesives. Indeed, Jorda et al. (2021) reported for epoxy, urea-
242 formaldehyde, melamine-urea-formaldehyde, phenol-formaldehyde and polyurethane resins
243 bonded five layer beech (*Fagus sylvatica*) plywood an MOE between 9,500 and 11,700 MPa, while
244 for MOR the values fall between 95 and 115 MPa[49]. Additionally, Biadala et al.[50] reported a mean
245 MOE of 13,720 MPa for three layered PF bonded beech plywood and a MOR of 158.4 MPa . Thus,
246 with an MOE over 13,000 MPa and MOR beyond 140 MPa, the co-polymers of furfuryl alcohol-
247 tannin-fibroin exhibit mechanical properties at least comparable to the main synthetic resins.
248
249 The morphology of the reference (TFS-0) and TSF-20 samples was investigated by SEM analysis
250 as reported in Figure 1C. The TFS-0 and TFS' show jagged morphology due to the fast evaporation
251 of formic acid during the crosslinking. On the contrary, the addition of RS (TFS-20 and TSF-20')
252 results in a more compact material. Salts crystals, e.g. $CaCl_2$, are visible, along with the appearance
253 of RS agglomerates (red cycle in Figure 1C, TFS-20' sample, and Figure S1 in SI section).

In order to understand and correlate the different formulations and their reactivity, a comparison between the reference and the silk-added samples were monitored through non-isothermal and isothermal TMA. In Figure 2, the thermomechanical behavior of formulations described in table 1 is reported. Focalizing on the non-isothermal method, heat affects the sample behaviors simultaneously in two different ways, namely by physical and chemical effects.[51] For the former an increase of temperature leads to the softening and decrease the stiffness of the polymers, which happens to all samples before 80°C. By raising the temperature, the chemical effect of cross-linking overcomes the physical one, and an increase in stiffness was registered between 80 and 180°C, due to the starting of the polymerization process.

Although all samples showed a maximum MOE peak around 180°C, the addition of RS shifts the starting of curing of about 10°C. This suggests (see below) that the addition of fibroin delays the co-polymerization of tannin and furfuryl alcohol. Once the curing process starts, the presence of fibroin accelerates the hardening and this can be seen by the slope of the thermograms which are particularly visible for the formulation containing at least 15wt% of RS. However, at the end of the polymerization process, the presence of silk increased the properties of the co-polymer. This result supports the observations already considered in the mechanical tests: in this case as well the TFS-20 registered the highest MOE compared to the other formulations.

The isothermal curves for the TFS-20 and TFS-0 (black and pink) are shown in Figure 2. After 240 min of reaction at room temperature, the reference (TFS-0, black curve) reached a higher MOE value than the TFS-20, indicating faster reaction kinetics. The acidity resulting from the presence of formic acid allows as for a fast self-polymerization[52] of furfuryl alcohol as well as a co-polymerization with tannin.[53]

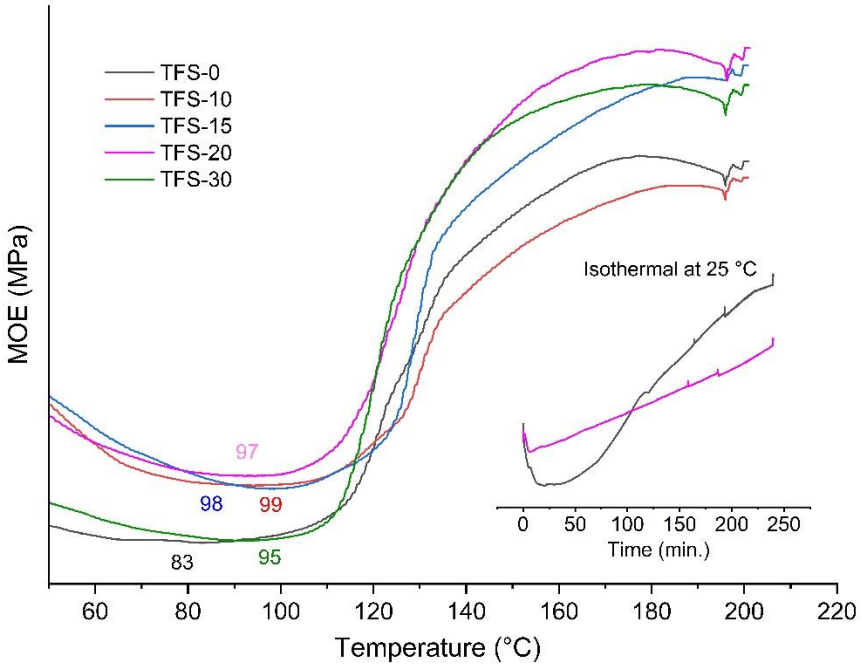


277

278 **Figure 2.** Non-isothermal and isothermal (see the inset) mechanical analysis of TSF-0 and TFS
279 samples synthesized at different wt% of RS.

280 $^{13}$C-NMR and ATR-FTIR analysis were performed to understand the chemical interactions
281 occurring between silk and the tannin-furanic matrix.

282 Many studies involved the characterization of the polyfurfuryl alcohol (PFA) since the last
283 century,[21,54,55] but the debate is still open due to its utilization as renewable and abundant material,
284 with more molecular rearrangements that have been proposed over the years.[25,56,57] In short there
285 are two reactions occurring: i) the linear polymerization summarized in the Scheme 1A and the ii)
286 Diels-Alder crosslinking of the ring-opened structures reported in Scheme 1B.

287

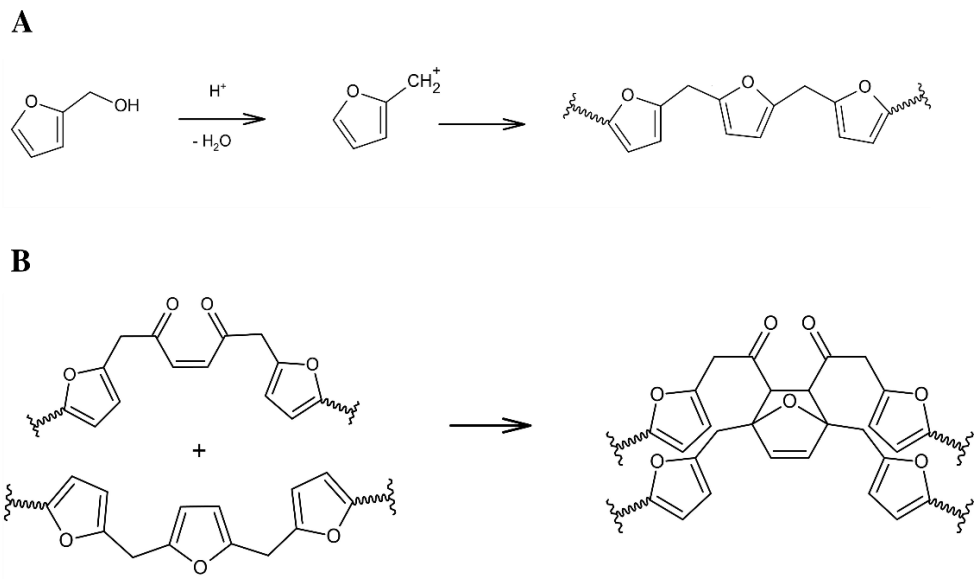


**Scheme 1.** A: Principal mechanism of reaction of furfuryl alcohol polymerization. B: Diels Alder reaction mechanism involved in the polymerization of furfuryl alcohol.

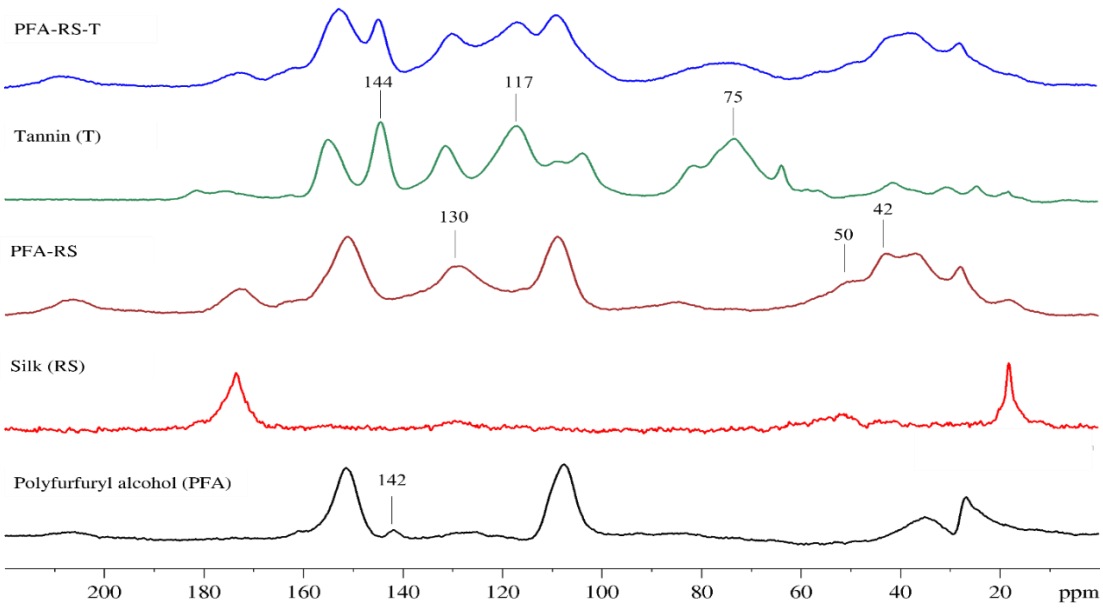


**Figure 3.** $^{13}$C-NMR spectra of: furfuryl alcohol (PFA, black curve), regenerated silk (RS, red curve), polyfurfuryl alcohol- regenerated silk (PFA-RS, brown ), quebracho tannin (T, green

294 curve) and quebracho polyfurfuryl alcohol-regenerated silk-quebracho tannin (PFA-RS-T, blue
295 curve).

296 In Figure 3 the $^{13}$C-NMR spectra of polyfurfuryl alcohol (PFA), regenerated silk (RS), PFA-RS,
297 quebracho tannin(T) and PFA-RS-T are reported. Comparing the spectra PFA and PFA-RS, it can
298 be seen that despite many signals are obtained by superposition of each component, new or highly
299 enhanced peaks were observed. Indeed, when silk is added (PFA-RS, brown curve), the band at
300 142 ppm disappears/strongly reduces its intensity, while the peak at around 130 ppm is severely
301 enhanced, and the signal at 50 ppm as well the shoulder at around 40 ppm appear. The signal at
302 142 ppm related to –C=C– in Diels-Alder bicycle[56] disappears, suggesting a decrease of the
303 cycloaddition crosslinking mechanism, while the enhancement of the signal at 130 ppm can be
304 attributed to the C=C of dienophile reagent (Scheme 1B), which is not involved anymore in Diels
305 Alder reaction. On the other hand, between 40 and 50 ppm a new signal is detected in the PFA-
306 RS spectrum, which is probably related to more substituted carbons (e.g. ternary carbon).[21,25]
307 Indeed, the acidity of the solution may lead to the formation of carbocation –$CH2^+$ in the primary
308 alcohol of sericin (Scheme 2A). The silk carbocation may interact with nucleophilic centers as
309 PFA linear conjugated system, whose presence is already confirmed by several authors [25,57,58],
310 leading to final three dimensional network represented in Scheme 2B. The coupling between those
311 two species could justify the resonance between 50 and 40 ppm which produces novel secondary
312 and ternary carbons. Furthermore, in support of what has just been hypothesized, Chen et al. have
313 recently confirmed the formation of covalent bonds between PFA and reactive functional groups
314 of gluten protein.[32]

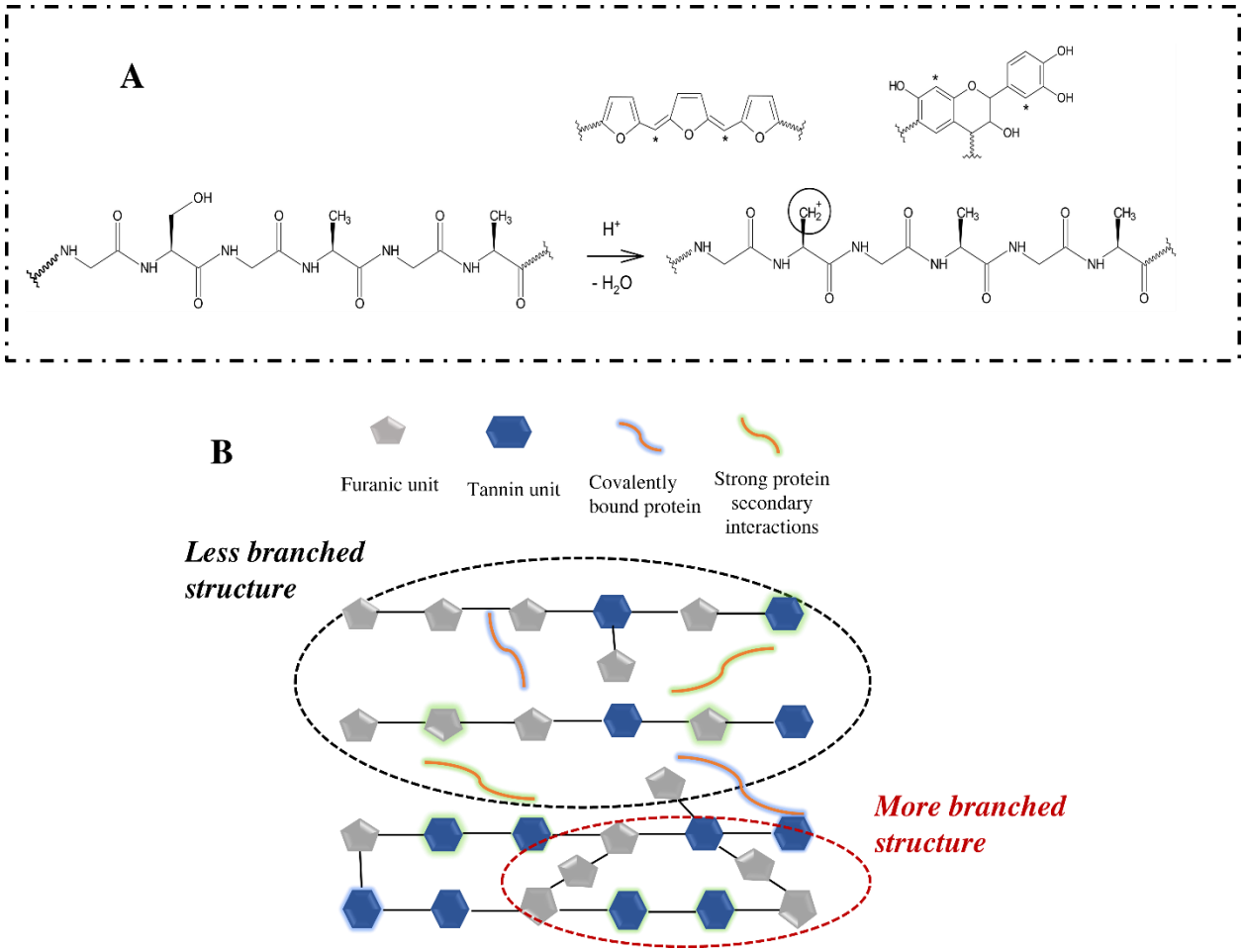


315

316 **Scheme 2.** A: possible carbocation formation in a primary alcohol of the silk protein structure and

317 interaction with nucleophilic centers*. B: schematic representation and possible interaction of a

318 tannin-alcohol furfuryl co-polymer and silk

319

320 The addition of tannin increases the complexity of the system and the overlapping of signals

321 does not facilitate the recognition of any new interactions. Definitely, the new peaks visible at 144

322 ppm, 117ppm and around 75 ppm are related to –C–O of B ring, –C–C– of A ring, and C aliphatic

323 involved in the polyphenolic structure.[18,53] On the other hand, the interaction of the silk carbocation

324 with the nucleophilic centers of the aromatic rings cannot be excluded (Scheme 2B). However, a

325 stable network between tannin and RS is also guaranteed by strong hydrogen and hydrophobic

interaction of those components[59]. Thus, the presence of the silk within network allow to more flexible and elastic system (black circle, Scheme 2B), which is not guaranteed without the protein due to the more branched final structure (red circle, Scheme 2B).

The samples were also investigated by ATR-FTIR spectroscopy. The spectra are reported in Figure 4.

The spectrum of PFA obtained in the present investigation shows several diagnostic signals already observed in a previous work, when PFA was prepared using a similar procedure.[56] The peaks at ca. 1520 $cm^{-1}$, 1420 $cm^{-1}$, 1013 $cm^{-1}$ and 785 $cm^{-1}$ can be ascribed to the linear PFA structure, while the bands at 1715 $cm^{-1}$, 1660 $cm^{-1}$ and 965 $cm^{-1}$ suggest the presence of the Diels-Alder product within the polymer matrix. [56] The spectrum of PFA-RS still evidences the signals related to the linear PFA structures at ca. 1520 $cm^{-1}$, 1013 $cm^{-1}$ and 785 $cm^{-1}$, the contribution at ca. 1715 $cm^{-1}$ due to the Diels-Alder product and the broad band at 965 $cm^{-1}$ related to ring-opened and/or Diels-Alder structures. Interestingly, it has been proposed that the presence of a contribution at ca. 735 $cm^{-1}$ might be used in conjunctions to the peak at 785 $cm^{-1}$ to estimate the relative amount of single-linked and double-linked furan rings within the PFA matrix. [57] In this respect, the spectra indicate that the relative intensity of the contribution at ca. 735 $cm^{-1}$ decreases going from PFA to PFA-RS, suggesting that the presence of silk reduces the relative fraction of single-linked furan rings. This is consistent with a silk-induced modulation of the cycloaddition crosslinking.

The spectrum of the PFA-RS-T sample is dominated by the tannin contribution; in any case the signals at 1013 $cm^{-1}$ (linear PFA), 965 $cm^{-1}$ (ring-opened and/or Diels-Alder PFA) and 785 $cm^{-1}$ (linear PFA) can be still recognized. Similarly to the case of the binary PFA-RS sample, a contribution at ca. 735 $cm^{-1}$ was not observed, in line with the idea that the silk mainly affects the polymerization process even in the ternary system.

To notice that a carbonyl resonance is still present in the spectrum (1715 $cm^{-1}$) of the PFA-RS-T sample (blue spectra, Figure 4). This might be attributed to the C=O stretching of both the formylated tannin and the Diels-Alder product. In order to obtain more information two samples crosslinked in formic acid (PFA-T and PFA-RS-T) were analyzed and the absorbance spectra obtained from FTIR imaging were compared. The relative analysis were compared, as reported in figure 5.

The integration ratio between the peak at 1715 $cm^{-1}$ (C=O) and at 1520 $cm^{-1}$ (C=C asymmetric stretching of tannin), is found to be 1.3 and 0.6 for PFA-T and PFA-RS-T, respectively. Thus, resulting in a decrease of more than 50% percent when RS is added to the PFA-tannin polymer.

This confirms that the addition of silk inhibits the Diels-Alder reaction. The protein chains fit into the polymer matrix by establishing secondary interactions, limiting the crosslinking to proceed. Due to the strong acidic environment, the formation of the covalent bonds between silk and furfuryl alcohol (proposed after $^{13}$C-NMR observation) cannot be excluded, the novel vibration of the $CH_2$-CH proposed would be overlapped (Stretching at around 3,000 and bending at below 1000 $cm^{-1}$) .

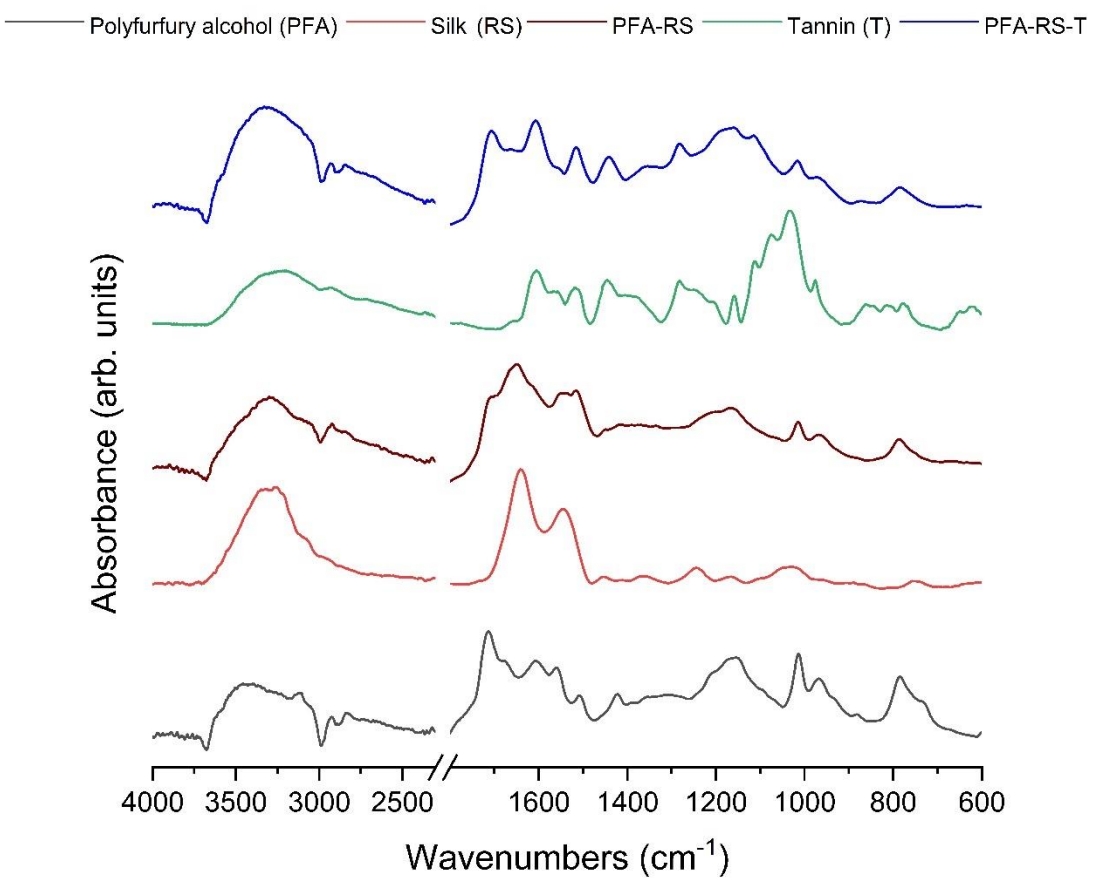


365

366 **Figure 4.** ATR-FT-IR spectra of: furfuryl alcohol (PFA, black curve), regenerated silk (RS, red
367 curve), polyfurfuryl alcohol-regenerated silk (PFA-RS, brown ), quebracho tannin (T, green
368 curve) and quebracho polyfurfuryl alcohol-regenerated silk-quebracho tannin (PFA-RS-T, blue
369 curve).

370

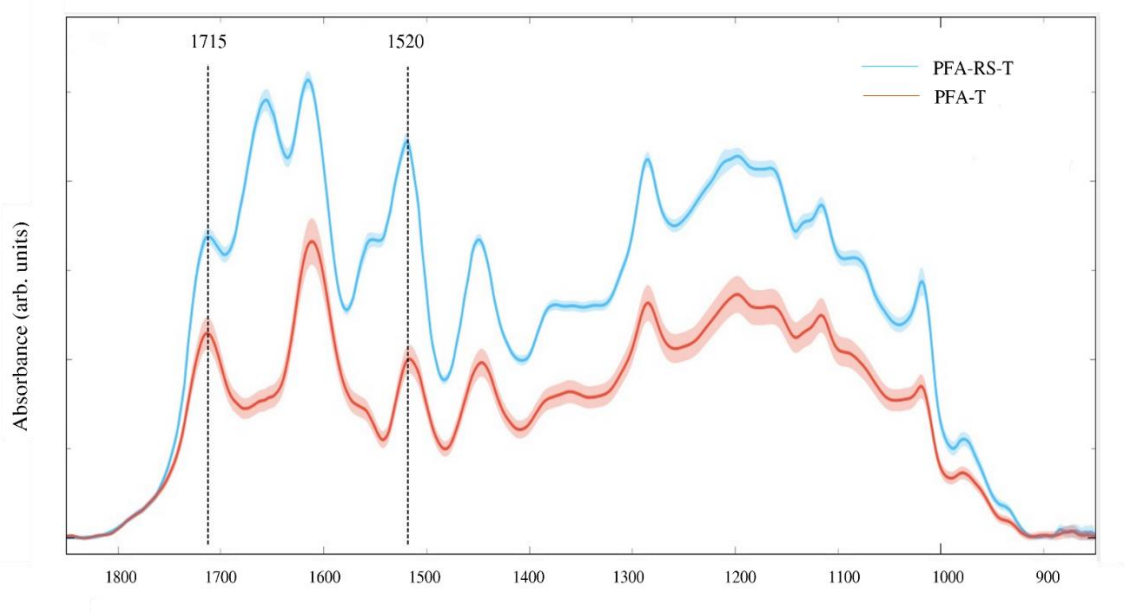


**Figure 5.** Average FTIR spectra of surface samples of polyfurfuryl alcohol-quebracho tannin (PFA-T, red curve) and polyfurfuryl alcohol-regenerated silk-quebracho tannin (PFA-RS-T, light blue curve).

## CONCLUSIONS

In this study RS was successfully added to tannin-furanic formulation to produce bio-based adhesives with enhanced mechanical properties. Significant enhancement of about 20-30% were observed in plywood gluing when 15-20 wt% of RS was added to the reference formulation in both dry and wet conditions.

These findings were rationalized considering that the presence of the RS limits the crosslinking of the furanic polymer resulting in a homogeneous network in which the presence of new chemical bonding between the silk and the furanic adduct are proposed.

This strategy provides a new approach to developing formaldehyde-free bio-based wood adhesive with rapid preparation, excellent performance, and sustainability. It was shown that the combination between vegetal and animal bioresources can cooperate synergically for the

production of performing wood adhesives. The interaction between silk, tannin and furanics can be considered also for other applications in the field of material science with particularly interesting perspectives in bio-plastic, construction composites and automotive but also in medical and biological devices.

## AUTHOR CONTRIBUTION

The manuscript was written through contributions of all authors. All authors have given approval to the final version of the manuscript.

## ACKNOWLEDGMENT

G.T. gratefully acknowledge the TESAF dept. for supporting this research with BIRD 2021 fundings "Biocomby-". E.C. thanks the LERH doctorate school for the grant financing his PhD. L.V. received funding from the Italian Ministry of Education, University and Research (MIUR) under the PRIN Project "Development and promotion of the Levulinic acid and Carboxylate platforms by the formulation of novel and advanced PHA-based biomaterials and their exploitation for 3D printed green-electronics applications" grant 2017FWC3WC.

## REFERENCE

(1) Söderholm, P. The green economy transition: The challenges of technological change for sustainability. *Sustain. Earth* **2020**, *3* (1), 6. https://doi.org/10.1186/s42055-020-00029-y.

(2) CIEL. Plastic & Climate: The hidden costs of a plastic planet; 2019. https://www.ciel.org/wp-content/uploads/2019/05/Plastic-and-Climate-FINAL-2019.pdf.

(3) Zheng, J.; Suh, S. Strategies to reduce the global carbon footprint of plastics. *Nat. Clim.*

*Chang.* **2019**, *9* (5), 374–378. https://doi.org/10.1038/s41558-019-0459-z.

(4) Spierling, S.; Knüpffer, E.; Behnsen, H.; Mudersbach, M.; Krieg, H.; Springer, S.; Albrecht, S.; Herrmann, C.; Endres, H. J. Bio-Based Plastics - A review of environmental, social and cconomic impact assessments. *J. Clean. Prod.* **2018**, *185*, 476–491. https://doi.org/10.1016/j.jclepro.2018.03.014.

(5) Rosenboom, J. G.; Langer, R.; Traverso, G. The hidden costs of a plastic planet. *Nat. Rev. Mater.* **2022**, *7* (2), 117–137. https://doi.org/10.1038/s41578-021-00407-8.

(6) Cesprini, E.; De Iseppi, A.; Giovando, S.; Tarabra, E.; Zanetti, M.; Šket, P.; Marangon, M.; Tondi, G. Chemical characterization of cherry (Prunus Avium) extract in comparison with commercial mimosa and chestnut tannins. *Wood Sci. Technol.* **2022**, 56, 1455-1473 https://doi.org/10.1007/s00226-022-01401-1.

(7) Shirmohammadli, Y.; Efhamisisi, D.; Pizzi, A. Tannins as a sustainable raw material for green chemistry: A review. *Ind. Crops Prod.* **2018**, *126*, 316–332. https://doi.org/10.1016/j.indcrop.2018.10.034.

(8) Falcão, L.; Araújo, M. E. M. Vegetable tannins used in the manufacture of historic leathers. *Molecules* **2018**, *23*, 8–10. https://doi.org/10.3390/molecules23051081.

(9) Cook, N. C.; Samman, S. Flavonoids - chemistry, metabolism, cardioprotective effects, and dietary Sources. *J. Nutr. Biochem.* **1996**, *7* (2), 66–76. https://doi.org/10.1016/0955-2863(95)00168-9.

(10) Eckardt, J.; Neubauer, J.; Sepperer, T.; Donato, S.; Zanetti, M.; Cefarin, N.; Vaccari, L.; Lippert, M.; Wind, M.; Schnabel, T.; Petutschnigg, A.; Tondi, G. Synthesis and

characterization of high-performing sulfur-free tannin foams. *Polymers (Basel).* **2020**, *12* (3), 564. https://doi.org/10.3390/polym12030564.

(11) Tondi, G.; Pizzi, A. Tannin-based rigid foams: characterization and modification. *Ind. Crops Prod.* **2009**, *29* (2–3), 356–363. https://doi.org/10.1016/j.indcrop.2008.07.003.

(12) Arbenz, A.; Avérous, L. Chemical modification of tannins to elaborate aromatic biobased macromolecular architectures. *Green Chem.* **2015**, *17* (5), 2626–2646. https://doi.org/10.1039/c5gc00282f.

(13) Sommerauer, L.; Thevenon, M. F.; Petutschnigg, A.; Tondi, G. Effect of hardening parameters of wood preservatives based on tannin copolymers. *Holzforschung* **2019**, *73* (5), 457–467. https://doi.org/10.1515/hf-2018-0130.

(14) Cesprini, E.; Baccini, R.; Urso, T.; Zanetti, M.; Tondi, G. Quebracho-based wood preservatives: effect of concentration and hardener on timber properties. *Coatings* **2022**, *12 (5)*, 568. https://doi.org/https:// doi.org/10.3390/coatings12050568.

(15) Pizzi, A. Recent developments in eco-efficient bio-based adhesives for Wìwood bonding: Opportunities and issues. *J. Adhes. Sci. Technol.* **2012**, 20 (8), 829-846.

(16) Hemmilä, V.; Adamopoulos, S.; Karlsson, O.; Kumar, A. Development of sustainable bio-adhesives for engineered wood panels-A review. *RSC Adv.* **2017**, *7* (61), 38604–38630. https://doi.org/10.1039/c7ra06598a.

(17) Pizzi, A. Tannins: Prospectives and actual industrial applications. *Biomolecules* **2019**, *9* (8), 344. https://doi.org/10.3390/biom9080344.

(18) Tondi, G. Tannin-based copolymer resins: Synthesis and characterization by solid state 13C

NMR and FT-IR spectroscopy. *Polymers (Basel).* **2017**, *9* (6), 223. https://doi.org/10.3390/polym9060223.

(19) Gandini, A. Polymers from renewable resources: a challenge for the future of macromolecular materials. *Macromolecules* **2008**, *41* (24), 9491–9504. https://doi.org/10.1021/ma801735u.

(20) Choura, M.; Belgacem, N. M.; Gandini, A. The acid-catalyzed polycondensation of furfuryl alcohol: old puzzles unravelled. *Macromol. Symp.* **1997**, *122*, 263–268. https://doi.org/10.1002/masy.19971220141.

(21) Choura, M.; Belgacem, N. M.; Gandini, A. Acid-catalyzed polycondensation of furfuryl alcohol: mechanisms of chromophore formation and cross-linking. *Macromolecules* **1996**, *29* (11), 3839–3850. https://doi.org/10.1021/ma951522f.

(22) Pfriem, A.; Dietrich, T.; Buchelt, B. furfuryl alcohol impregnation for improved plasticization and fixation during the densification of wood. *Holzforschung* **2012**, *66* (2), 215–218. https://doi.org/10.1515/HF.2011.134.

(23) Kong, L.; Guan, H.; Wang, X. In situ polymerization of furfuryl alcohol with ammonium dihydrogen phosphate in poplar wood for improved dimensional stability and flame retardancy. *ACS Sustain. Chem. Eng.* **2018**, *6* (3), 3349–3357. https://doi.org/10.1021/acssuschemeng.7b03518.

(24) Yao, M.; Yang, Y.; Song, J.; Yu, Y.; Jin, Y. Lignin-based catalysts for chinese fir furfurylation to improve dimensional stability and mechanical properties. *Ind. Crops Prod.* **2017**, *107* (May), 38–44. https://doi.org/10.1016/j.indcrop.2017.05.038.

(25) Falco, G.; Guigo, N.; Vincent, L.; Sbirrazzuoli, N. Opening furan for tailoring properties of bio-based poly(furfuryl alcohol) thermoset. *ChemSusChem* **2018**, *11* (11), 1805–1812. https://doi.org/10.1002/cssc.201800620.

(26) Luckeneder, P.; Gavino, J.; Kuchernig, R.; Petutschnigg, A.; Tondi, G. Sustainable phenolic fractions as basis for furfuryl alcohol-based co-polymers and their use as wood adhesives. *Polymers (Basel).* **2016**, *8* (11). https://doi.org/10.3390/polym8110396.

(27) Szczurek, A.; Fierro, V.; Thébault, M.; Pizzi, A.; Celzard, A. Structure and properties of poly(furfuryl alcohol)-tannin polyHIPEs. *Eur. Polym. J.* **2016**, *78*, 195–212. https://doi.org/10.1016/j.eurpolymj.2016.03.037.

(28) Cesprini, E.; Causin, V.; Iseppi, A. De; Zanetti, M.; Marangon, M.; Barbu, M. C.; Tondi, G. Renewable tannin-based adhesive from Quebracho extract and furfural for particleboards. *Forest.* **2022**, 3–5.

(29) Jorda, J.; Cesprini, E.; Barbu, M.-C.; Tondi, G.; Zanetti, M.; Král, P. Quebracho tannin bio-based adhesives for plywood. *Polymers (Basel).* **2022**, *14* (11), 2257. https://doi.org/10.3390/polym14112257.

(30) Zhang, J.; Long, C.; Zhang, X.; Liu, Z.; Zhang, X.; Liu, T.; Li, J.; Gao, Q. An easy-coating, versatile, and strong soy flour adhesive via a biomineralized structure combined with a biomimetic brush-like polymer. *Chem. Eng. J.* **2022**, *450* (P4), 138387. https://doi.org/10.1016/j.cej.2022.138387.

(31) Xu, Y.; Han, Y.; Li, J.; Luo, J.; Shi, S. Q.; Li, J.; Gao, Q.; Mao, A. Research progress of soybean protein adhesive: a review. *J. Renew. Mater.* **2022**, *10* (10), 2519–2541.

https://doi.org/10.32604/jrm.2022.020750.

(32) Chen, X.; Yang, Z.; Yang, F.; Pizzi, A.; Essawy, H.; Du, G.; Zhou, X. development of easy-handling, formaldehyde-free, high-bonding performance bio-sourced wood adhesives by co-reaction of furfuryl alcohol and wheat gluten protein. *J. Chem. Eng.J.* **2023**, *462*, 142161. https://doi.org/10.2139/ssrn.4281052.

(33) Zhao, X.; Liu, T.; Ou, R.; Hao, X.; Fan, Q.; Guo, C.; Sun, L.; Liu, Z.; Wang, Q. Fully Biobased Soy Protein Adhesives with Integrated High-Strength, Waterproof, Mildew-Resistant, and Flame-Retardant Properties. *ACS Sustain. Chem. Eng.* **2022**, *10* (20), 6675–6686.

(34) Cao, Z.; Chen, X.; Yao, J.; Huang, L.; Shao, Z. The preparation of regenerated silk fibroin microspheres. *Soft Matter* **2007**, *3* (7), 910–915. https://doi.org/10.1039/b703139d.

(35) Ceccarini, M. R.; Palazzi, V.; Salvati, R.; Chiesa, I.; Maria, C. De; Bonafoni, S.; Mezzanotte, P.; Codini, M.; Pacini, L.; Errante, F.; Rovero, P.; Morabito, A.; Beccari, T.; Roselli, L.; Valentini, L. Biomaterial inks from peptide-functionalized silk fibers for 3D printing of futuristic wound-healing and sensing materials. **2023**. 24(2), 947; https://doi.org/10.3390/ijms24020947

(36) Santoni, I.; Pizzo, B. Evaluation of alternative vegetable proteins as wood adhesives. *Ind. Crops Prod.* **2013**, *45*, 148–154. https://doi.org/10.1016/j.indcrop.2012.12.016.

(37) Raydan, N. D. V.; Leroyer, L.; Charrier, B.; Robles, E. Recent advances on the development of protein-based adhesives for wood composite materials—a review. *Molecules* **2021**, *26* (24). https://doi.org/10.3390/molecules26247617.

(38) Valentini, L.; Ceccarini, M. R.; Verdejo, R.; Tondi, G.; Beccari, T. Stretchable, bio-compatible, antioxidant and self-powering adhesives from soluble silk fibroin and vegetal polyphenols exfoliated graphite. *Nanomaterials* **2021**, *11* (9). https://doi.org/10.3390/nano11092352.

(39) British Standards, E. B. Plywood — Bonding Quality — EN 314-1:2004. **2004**, *3*.

(40) British Standards, E. B. Wood-Based Panels — Determination of Modulus of Elasticity in Bending and of Bending Strength- EN 310:1993. **1993**, 1–14.

(41) Toplak, M.; Read, S. T.; Sandt, C.; Borondics, F. Quasar: easy machine learning for biospectroscopy. *Cells* **2021**, *10* (9), 1–10. https://doi.org/10.3390/cells10092300.

(42) Toplak, M.; Birarda, G.; Read, S.; Sandt, C.; Rosendahl, S. M.; Vaccari, L.; Demšar, J.; Borondics, F. Infrared orange: connecting hyperspectral data with machine learning. *Synchrotron Radiat. News* **2017**, *30* (4), 40–45. https://doi.org/10.1080/08940886.2017.1338424.

(43) Xi, X.; Pizzi, A.; Frihart, C. R.; Lorenz, L.; Gerardin, C. Tannin plywood bioadhesives with non-volatile aldehydes generation by specific oxidation of mono- and disaccharides. *Int. J. Adhes. Adhes.* **2020**, *98*. https://doi.org/10.1016/j.ijadhadh.2019.102499.

(44) Liu, Z.; Chen, M.; Xu, Y.; Zhang, J.; Huang, X.; Luo, J.; Li, J.; Shi, S. Q.; Gao, Q. Preparation of a strong and multiple-function soybean flour adhesive via the construction of tannin microspheres with a core–shell structure. *Compos. Part B Eng.* **2022**, *242* (February), 110114. https://doi.org/10.1016/j.compositesb.2022.110114.

(45) Zhou, Y.; Zeng, G.; Zhang, F.; Tang, Z.; Luo, J.; Li, K.; Li, X.; Li, J.; Shi, S. Q. Preparation

of functional fiber hybrid enhanced high strength and multifunctional protein based adhesive. *Mater. Des.* **2022**, *224*, 111289. https://doi.org/10.1016/j.matdes.2022.111289.

(46) Pang, H.; Zhao, S.; Mo, L.; Wang, Z.; Zhang, W.; Huang, A.; Zhang, S.; Li, J. Mussel-inspired bio-based water-resistant soy adhesives with low-cost dopamine analogue-modified silkworm silk fiber. *J. Appl. Polym. Sci.* **2020**, *137* (23), 1–10. https://doi.org/10.1002/app.48785.

(47) Liu, Z.; Liu, T.; Jiang, H.; Zhang, X.; Li, J.; Shi, S. Q.; Gao, Q. Biomimetic lignin-protein adhesive with dynamic covalent/hydrogen hybrid networks enables high bonding performance and wood-based panel recycling. *Int. J. Biol. Macromol.* **2022**, *214* (April), 230–240. https://doi.org/10.1016/j.ijbiomac.2022.06.042.

(48) Hafiz, N. L. M.; Tahir, P. M. D.; Hua, L. S.; Abidin, Z. Z.; Sabaruddin, F. A.; Yunus, N. M.; Abdullah, U. H.; Abdul Khalil, H. P. S. Curing and thermal properties of co-polymerized tannin phenol-formaldehyde resin for bonding wood veneers. *J. Mater. Res. Technol.* **2020**, *9* (4), 6994–7001. https://doi.org/10.1016/j.jmrt.2020.05.029.

(49) Jorda, J.; Kain, G.; Barbu, M. C.; Petutschnigg, A.; Král, P. Influence of adhesive systems on the mechanical and physical properties of flax fiber reinforced beech plywood. *Polymers (Basel).* **2021**, *13* (18), 1–15. https://doi.org/10.3390/polym13183086.

(50) Biadala, T.; Czarnecki, R.; Dukarska, D. Water resistant plywood of increased elasticity produced from european wood species. *Wood Res.* **2020**, *65* (1), 111–123. https://doi.org/10.37763/wr.1336-4561/65.1.111124.

(51) Lei, H.; Frazier, C. E. Curing behavior of melamine-urea-formaldehyde (MUF) resin

adhesive. *Int. J. Adhes. Adhes.* **2015**, *62*, 40–44. https://doi.org/10.1016/j.ijadhadh.2015.06.013.

(52) Cefarin, N.; Bedolla, D. E.; Surowka, A.; Donato, S.; Sepperer, T.; Tondi, G.; Dreossi, D.; Sodini, N.; Birarda, G.; Vaccari, L. Study of the spatio-chemical heterogeneity of tannin-furanic foams: From 1D FTIR spectroscopy to 3D FTIR micro-computed tomography. *Int. J. Mol. Sci.* **2021**, *22* (23) 12869. https://doi.org/10.3390/ijms222312869.

(53) Cesprini, E.; Šket, P.; Causin, V.; Zanetti, M.; Tondi, G. Development of Quebracho ( Schinopsis Balansae ) tannin-based thermoset resins. **2021**, *13(24)*, 4412.

(54) Conley, R.; Metil, I. An investigation of the structure of furfuryl alcohol polycondensates with infrared spectroscopy. Reinhold Publishing Corporation, New York, 1963. https://doi.org/10.1002/app.1963.070070104.

(55) Myers, G. E. 13C NMR Study of curing in furfuryl alcohol resins. *Macromolecules* **1984**, *17*, 1087–1090.

(56) Tondi, G.; Cefarin, N.; Sepperer, T.; D'Amico, F.; Berger, R. J. F.; Musso, M.; Birarda, G.; Reyer, A.; Schnabel, T.; Vaccari, L. Understanding the polymerization of polyfurfuryl alcohol: ring opening and diels-alder reactions. *Polymers (Basel).* **2019**, *11* (12), 1–15. https://doi.org/10.3390/polym11122126.

(57) D'Amico, F.; Musso, M. E.; Berger, R. J. F.; Cefarin, N.; Birarda, G.; Tondi, G.; Bertoldo Menezes, D.; Reyer, A.; Scarabattoli, L.; Sepperer, T.; schnabel, t.; vaccari, l. chemical constitution of polyfurfuryl alcohol investigated by FTIR and resonant Raman spectroscopy. *Spectrochim. Acta - Part A Mol. Biomol. Spectrosc.* **2021**, *262* (June),

120090. https://doi.org/10.1016/j.saa.2021.120090.

(58) Buchwalter, S. L. Polymerization of furfuryl acetate in acetonitrole. *J. Polym. Sci. A1.* **1985**, *23* (12), 2897–2911. https://doi.org/10.1002/pol.1985.170231202.

(59) Ma, M.; Dong, S.; Hussain, M.; Zhou, W. Effects of addition of condensed tannin on the structure and properties of silk fibroin film. *Polym. Int.* **2017**, *66* (1), 151–159. https://doi.org/10.1002/pi.5272.